



OPEN ACCESS

Joseph E. Borovsky, Space Science Institute (SSI), United States

Megha Pandya, NASA Goddard Space Flight Center, United States Shipra Sinha. NASA Goddard Space Flight Center. **United States**

*CORRESPONDENCE Kun Li.

□ likun37@mail.sysu.edu.cn

RECEIVED 11 August 2025 REVISED 31 October 2025 ACCEPTED 05 November 2025 PUBLISHED 26 November 2025

CITATION

Li K, Chen J, Chai L, Kronberg E and Doepke N (2025) Evolution of the electron-to-ion temperature ratio of cold plasma in the lobes. Front, Astron. Space Sci. 12:1683785. doi: 10.3389/fspas.2025.1683785

© 2025 Li, Chen, Chai, Kronberg and Doepke. This is an open-access article distributed under the terms of the Creative Commons Attribution License (CC BY). The use. distribution or reproduction in other forums is permitted, provided the original author(s) and the copyright owner(s) are credited and that the original publication in this journal is cited, in accordance with accepted academic practice. No use, distribution or reproduction is permitted which does not comply with these terms.

Evolution of the electron-to-ion temperature ratio of cold plasma in the lobes

Kun Li^{1*}, Junhan Chen¹, Lihui Chai², Elena Kronberg³ and Nicolas Doepke³

¹Planetary Environmental and Astrobiological Research Laboratory, School of Atmospheric Sciences, Sun Yat-sen University, Zhuhai, China, ²Institute of Geology and Geophysics, Chinese Academy of Sciences, Beijing, China, ³Department of Earth and Environmental Sciences, Ludwig-Maximilians-Universität München, Munich, Germany

Cold plasma of ionospheric origin, with energies less than a few tens of electronvolts, dominates the plasma population in the magnetosphere and plays a crucial role in magnetospheric dynamics. Although the velocity distribution of cold plasma in the magnetotail is measured, little is known about the changes in its temperatures because of the difficulty in directly measuring the cold plasma. In this study, we examine the electric field measurements in the plasma wake, which is created by charged spacecraft interacting with the cold plasma flow, to infer the changes in the electron-to-ion temperature ratio of the cold plasma. We present observations from the Cluster mission during the years 2001–2010 and the distributions of the observed electric potential decrease in the plasma wake. The results confirm the correlation between the wake potential and the plasma flow speed and indicate that the electron-to-ion temperature ratio of the cold plasma decreases with increasing geocentric distance, suggesting that electrons are heated differently from ions as the cold plasma is transported into the tail.

KEYWORDS

cold plasma, temperature ratio, spacecraft potential, magnetotail lobes, plasma wake

1 Introduction

The plasma in the Earth's magnetotail lobes primarily originates from the ionospheric polar wind, consisting of ions and electrons with energies and temperatures below a few tens of electronvolts (André et al., 2015; Engwall et al., 2009), and is often referred to as cold plasma. Ions in the cold plasma are accelerated by an ambipolar electric field generated by faster moving electrons (Axford, 1968; Collinson, 2024) in the topside ionosphere and escape together with electrons along the open field lines of the polar region. Cold plasma has been confirmed (Haaland et al., 2012; Nilsson et al., 2010) to be further accelerated by the centrifugal force in the tail lobes as it flows into the tail.

The lobe magnetic fields that connect the tail and the ionosphere act as a waveguide for Alfvén waves. Alfvén waves in the lobes are known to interact with ionospheric outflow (Keiling et al., 2005; Takada et al., 2006; Sauvaud et al., 2004); it remains unclear how significantly the electrons and ions of the cold outflowing plasma are heated. To address this question, it is important to measure the electron-to-ion temperature ratio of cold plasma.

The main difficulty in measuring the cold ion temperature arises from the spacecraft's electric potential, which is normally positive for spacecraft in a sunlit and tenuous plasma

environment. The spacecraft's potential is large enough to repel cold ions, preventing them from being measured using the ion spectrometers onboard the spacecraft.

An alternative is to use the *in situ* electric field measurements. As the cold plasma has a bulk kinetic energy larger than its thermal energy, it is often supersonic in the lobes. When a spacecraft encounters the cold plasma in the lobes, a plasma wake downstream of the spacecraft with an imbalanced electric charge distribution is formed. For more details on the plasma wake, we refer to André et al. (2021).

Figure 1 shows the examples of wake detection during a lobe crossing by Cluster 3. Figure 1a shows the magnetic field measurements made using the fluxgate magnetometer (FGM) (Balogh et al., 2001). From the X-component of the B-field, it is observed that the spacecraft moved from the northern lobe to the central plasma sheet before joining the southern lobe. Figure 1b shows the plasma β value calculated from the ratio of the proton pressure, measured using a cluster ion spectrometer (CIS) (Rème et al., 2001), to the magnetic field pressure. The lobes are often defined as the region with plasma β less than 1. In this case, the measurements before 21 September 2001 23:00 and after 22 September 2001 07:00 were in the northern and southern lobes, respectively. The red dots in this panel indicate the time periods in which the plasma wake was detected. Note that the wake was detected only in the lobes because highenergy ions in other regions are unaffected by the spacecraft potential and by ramming into the wake. These high-energy ions neutralize the electric charge in the wake and erase the wake signature. The lobes filled with cold plasma are suitable for the wake formation.

The wake detection relies on observations from the electric-field and wave experiment (EFW) (Gustafsson et al., 1997) and the electron drift instrument (EDI) (Paschmann et al., 2001) onboard the Cluster spacecraft. Figures 1c–e show the electric-field measurements during a period of the lobe crossing that is marked by the vertical lines in Figures 1a,b. As the probe pair of EFW corotates with the spinning Cluster spacecraft, the potential difference between the two probes separated by 88 m produces a periodic signal. The electric field between probes 3 and 4 (E_{34}) of the EFW is shown as the blue curve in Figure 1c. The spacecraft-scale electric field measured from EFW differs from the background electric field measured using EDI. The orange curve in Figure 1c represents the background electric field projected along the 34 probe pair of the EFW (E_{EDI}^*).

Following Engwall et al. (2006) and André et al. (2015), the wake electric field is identified when the maximal discrepancy between two instruments (E^{W*}) in a 4-s spin period exceeds 2 mV/m (Figure 1d). The profile of E^{W*} is reproduced by the simulation of Engwall et al. (2006) (their Figure 6). Figure 1e shows the wake depth Φ^W , defined as the maximal potential difference between EFW probes 3 and 4 per spin period.

 Φ^W varies with the ion flow Mach number and the electron-to-ion temperature ratio, which are discussed in Section 2. Section 3 presents useful data selected from the previously derived cold plasma dataset presented by André et al. (2015). Section 4 illustrates the statistical results, which are followed by discussions and conclusions.

2 Inferring the temperature ratio from the wake depth measurements

This section summarizes the main factors that affect the wake depth measurements and show how the temperature ratio is inferred.

2.1 Φ^W modulated by the Mach number

For simplicity, we first consider the situation under which a spacecraft has a neutral surface charge. According to theoretical calculations by Alpert et al. (1965) and André et al. (2021), the wake depth is influenced by the ion flow Mach number (M):

$$M = \sqrt{\frac{m_i u^2}{2KT_i}},\tag{1}$$

where m_i and T_i are the ion mass and the ion temperature, respectively. u is the speed of the ion flow relative to the spacecraft, and K is the Boltzmann constant. In simulations by André et al. (2021), Φ^W increases monotonically with M, particularly when the plasma flow lies in the spin plane of the spacecraft.

2.2 Φ^W modulated by the temperature ratio

The wake depth is also influenced by the electron-to-ion temperature ratio of the background plasma $(r_T = T_e/T_i)$, particularly when the spacecraft acquires a positive surface potential (V_{SC}) due to the photoelectron effect. In the lobes, the following condition is often satisfied: $KT_i < \frac{m_i u^2}{2} < eV_{SC}$. Under such conditions, electrons attracted by the spacecraft potential can more easily fill the wake, whereas ions are repelled by the positive spacecraft potential and tend to scatter. As a result, a wake with electron density higher than ion density is formed. The wake is much wider than the geometric size of the spacecraft (2.2 m) in diameter), and Φ^W is expected to increase with higher values of r_T .

Engwall et al. (2006) carried out numerical simulations using a constant u of 20 km/s relative to the Cluster spacecraft. These simulations incorporate the material properties of the Cluster spacecraft surface, along with background plasma parameters such as density, bulk velocity, and electron and ion temperatures. A range of temperature combinations and plasma densities were tested to assess their influence on the plasma wake. Table 1 summarizes their simulation results. The length (L), width (W), and height (H) of the wake are modulated by multiple parameters, including V_{SC} , background plasma density (n_0) , T_e , and T_i . As expected, the larger the T_i value, the smaller the wake size, for the same T_e and V_{SC} . The boundary of the wake is defined by the surface where the ion density decreased to 75% of the background density.

Their simulations indicate that r_T is the main controlling factor for Φ^W . In Table 1, Φ^W increases monotonically from 0.23 V to 0.60 V as r_T increases from 0.5 to 2.0. This is expected because the higher the r_T value, the more electrons fill the wake, resulting in a larger Φ^W . With $r_T = 1$, the simulated Φ^W with changes in other

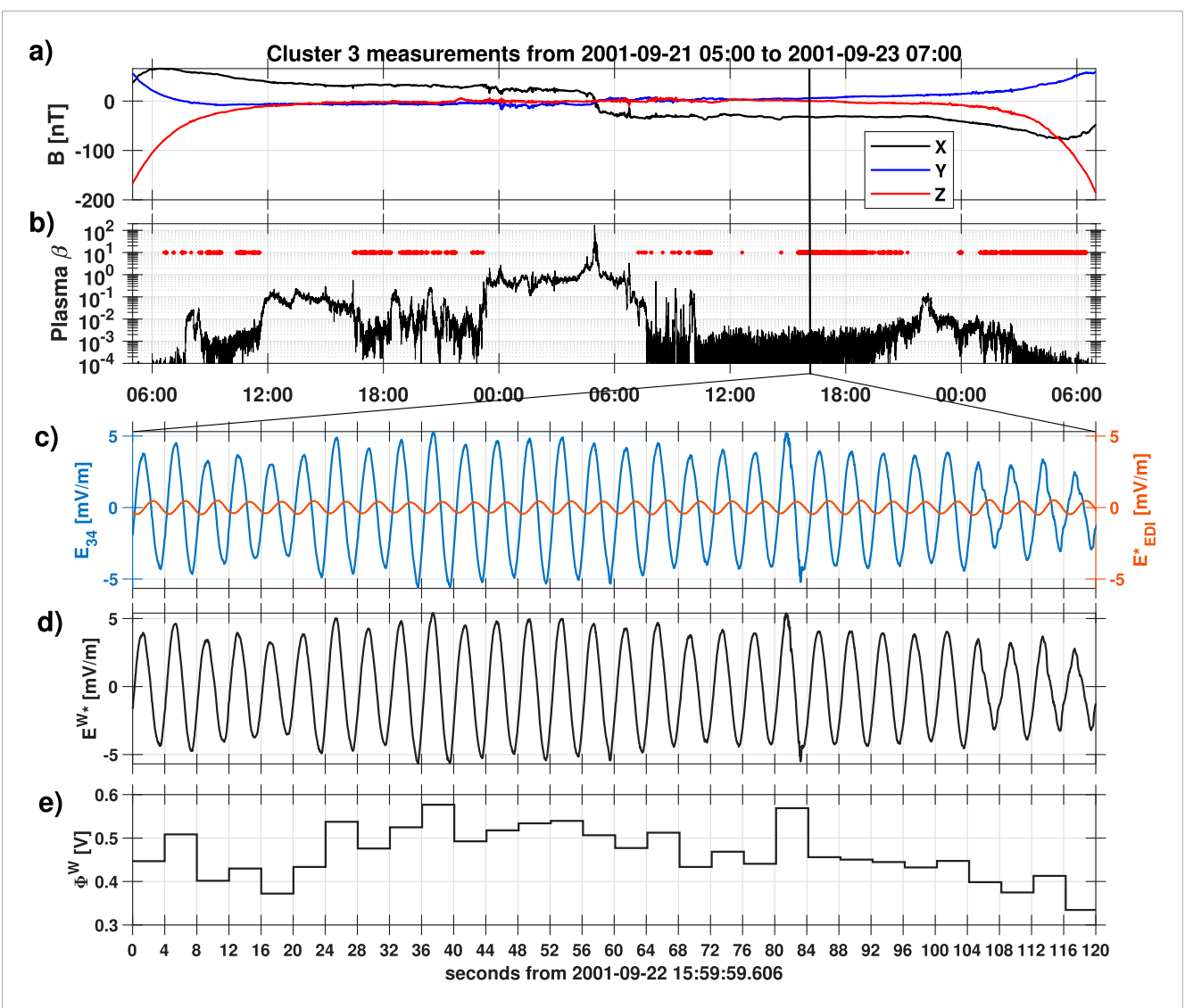
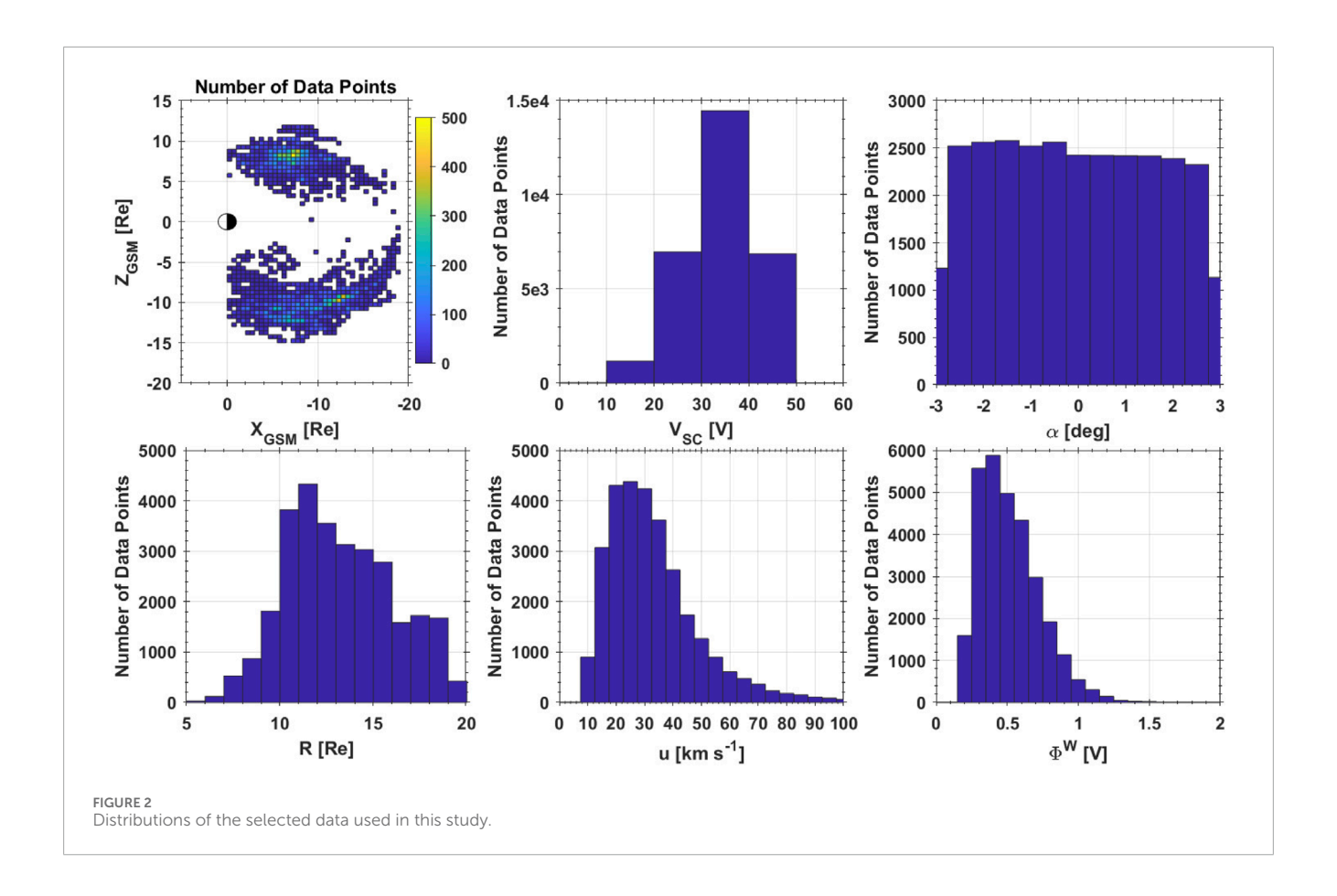


FIGURE 1
Example of plasma wake detection during a lobe crossing by Cluster 3. (a) In situ magnetic field in the Geocentric Solar Ecliptic coordinates measured using the FGM instrument. (b) Plasma beta calculated from the CIS data (black curve) and periods in which the plasma wake was detected (red dots). (c) Electric fields measured using the EFW (spacecraft-scale) and the EDI (background). (d) Electric field derived from the differences in the measurements between the two electric field instruments (E^{W*}). (e) The wake depth (Φ^{W}), defined as the maximum potential difference between the probes 3 and 4 in one spin period, calculated from the maximum values of E^{W*} multiplied by the separation between the probes 3 and 4.

TABLE 1 Values of Φ^W and dimensions of the wake from the simulations by Engwall et al. (2006), with different ion and electron temperatures and background plasma density (n_0) . In these simulations, u was set as $u = 20 \ km/s$.

Simulation	n ₀ [cm ⁻³]	<i>V_{sc}</i> [<i>V</i>]	KT _e [eV]	KT _i [eV]	r _T	$\Phi^W[V]$	L [m]	W [m]	H [m]
1	0.20	35	2.0	2.0	1.0	0.37	132	97	96
2	0.20	35	1.0	1.0	1.0	0.39	143	84	78
3	0.20	35	2.0	1.0	2.0	0.60	170	111	107
4	0.20	35	1.0	2.0	0.5	0.23	81	62	58
5	0.40	20	2.0	2.0	1.0	0.32	86	68	62
6	0.40	20	1.0	1.0	1.0	0.35	97	57	53



parameters (n_0 , V_{SC} , T_e , and T_i) has much smaller variation, between 0.32 and 0.39.

Therefore, Φ^W increases with both M and r_T . As u has a higher power number than T_i in Equation 1 and u ranges from 10 to 100 km/s (see Figure 2), changes in M are mainly considered to be caused by variations in u. As a result, u can serve as a proxy for M. We have the following Equation 2:

$$\Phi^W \propto (u, r_T). \tag{2}$$

The dataset derived from the Cluster mission contains the measurements of u and Φ^W . By comparing the measured Φ^W with the simulated Φ^W in Table 1, r_T of the cold plasma with u=20km/s (the most frequently measured) can be inferred. The positive correlation between r_T and Φ^W holds for other ranges of u, although a quantitative inference of r_T is not feasible for every range of u.

3 Data

The cold ion dataset used in this study includes measurements of the wake electric field, which has been used to derive the bulk flow velocity of ions with energies of a few tens of eV. For details of the dataset, we refer to Engwall et al. (2009) and André et al. (2015). Numerous studies have used this dataset to investigate the characteristics of the ionospheric outflow. For a comprehensive overview of the wake method and related research, we refer readers to the reviews by André et al. (2021) and Li et al. (2021).

The data include both the wake depth (Φ^W) and the elevation angle (α) , defined as the angle between the plasma flow velocity and the spin plane of the spacecraft. In total, approximately 330,000 data points with 4-s time resolution were collected by Cluster 1 between 2001 and 2009 and by Cluster 3 from 2001 to 2010 (excluding the year 2006). The data span the months from July to November each year, during which the spacecraft operated within the magnetosphere.

To ensure that the plasma flow lies in the spin plane and that the measurement of the wake depth is reliable, we used a maximum elevation angle $\alpha_{max} = 3^{\circ}$ to select the data. This value ensures a large enough number of data points. We note that our results do not change when using a smaller α_{max} , such as $\alpha_{max} = 1^{\circ}$. This is reasonable because the probes on both ends of the boom wire were always inside the wake during the entire spin period, with a relatively large elevation angle. As simulated by Engwall et al. (2006), the wake size is much larger than the 44-m-long boom wire of the EFW instrument. After selection, there are approximately 29,500 data points for further analysis.

4 Results

Figure 2 shows the distributions of the selected data. Measurements were made in a large part of the tail lobes, with values of R ranging from 6 to 20 Re. The dataset contains only the measurements in the lobes and the polar cap region because

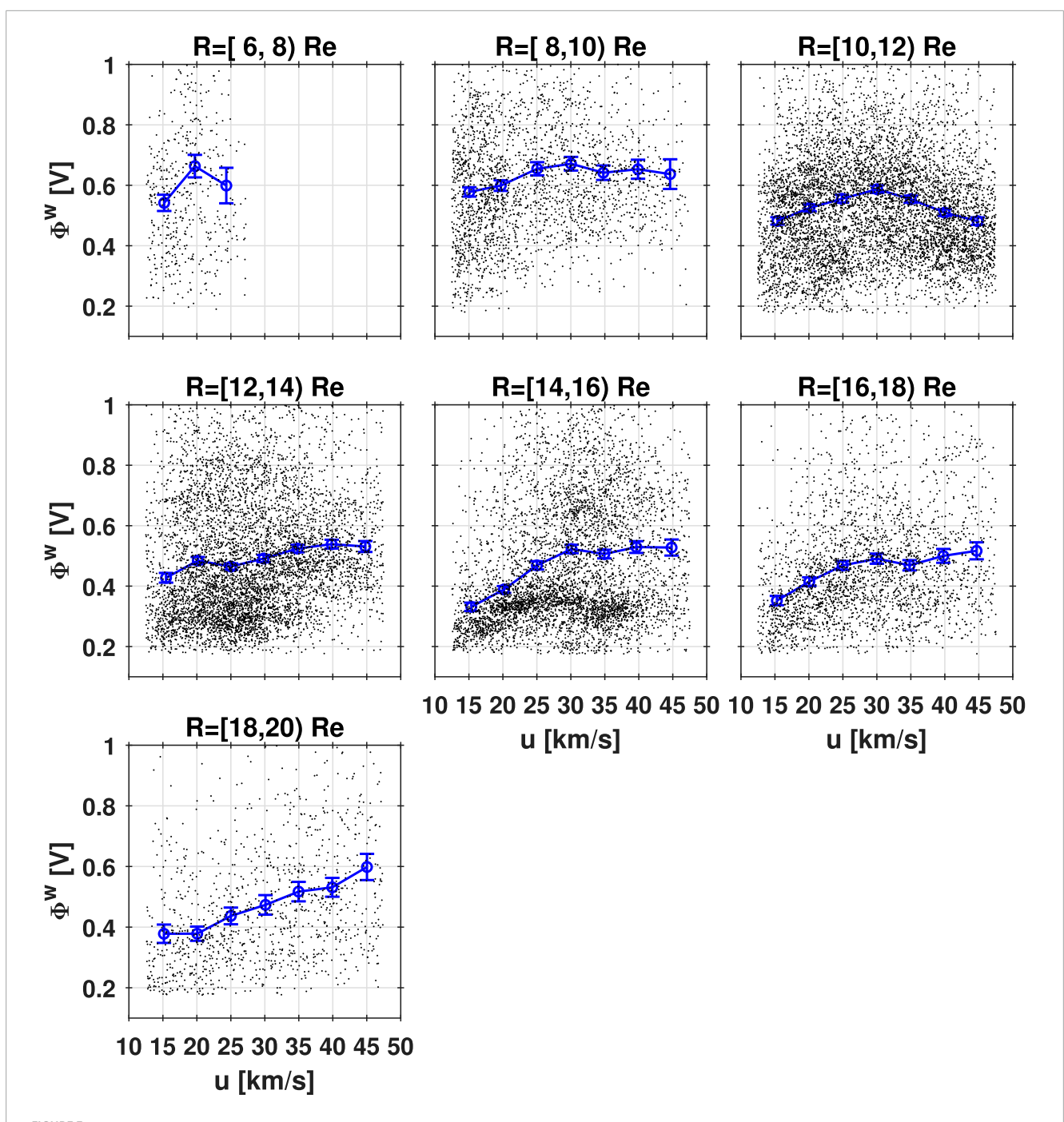
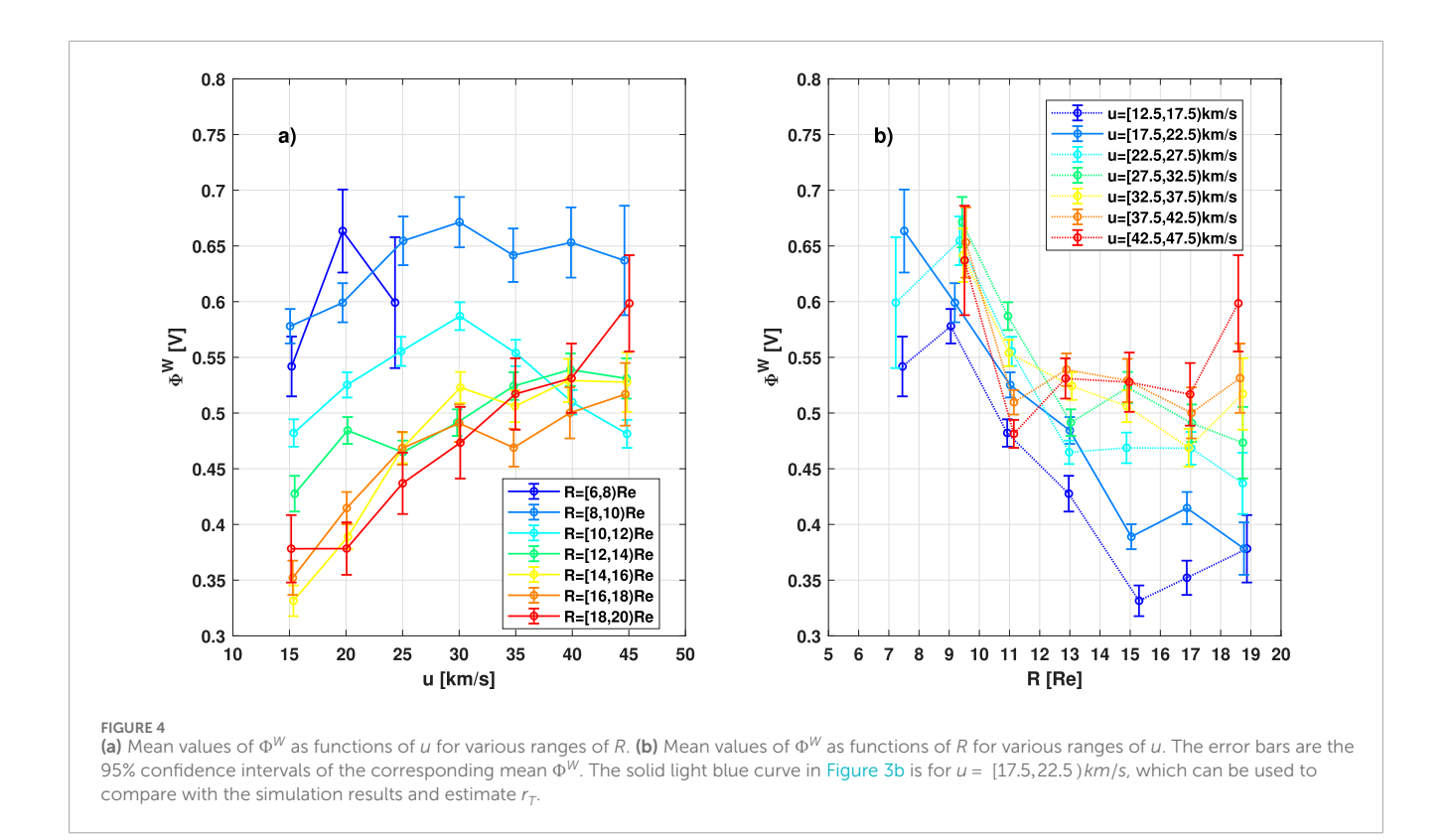


FIGURE 3 Correlation between Φ^W and u for different ranges of R. In each panel, the black dot represents each individual measurement. Blue circles and error bars are the mean values and the corresponding 95% confidence intervals, respectively. All the mean values are calculated from at least 30 measurements of Φ^W .

the enhanced wake cannot be formed in the high-energy particle environment. The ion flow speed relative to the spacecraft (u) has a mean value of 33 km/s. These distributions are similar to those before selection shown by André et al. (2015). The measured Φ^W ranges from 0.2 to 1.5 V, with values most frequently at approximately 0.4 V.

4.1 Effects of u on Φ^W

Figure 3 shows the measured Φ^W (black dots) as a function of the plasma flow speed relative to the spacecraft for various ranges of geocentric distance. The x- and y-coordinates of the blue circles denote the mean values of u and Φ^W , respectively, within each



corresponding range of u binned at 5 km/s intervals. The error bars mark the corresponding 95% confidence interval. Φ^W is observed to be positively correlated with u for most geocentric distance ranges.

The positive correlation between u and Φ^W is expected from the calculations of André et al. (2021) for the narrowed wake without the spacecraft potential described in Section 1. To study the spatial distribution of r_T , we need to remove the effects of u by analyzing the measurements with the same u.

4.2 Correlation between r_T and R

Since the spacecraft acquired a positive electric potential, the size of the wake observed in our study is enhanced. In addition to u, Φ^W is affected by r_T . This may explain why the trends in Figure 3 differ from the calculations shown in Figure 3b of André et al. (2021).

In Figure 3a, we combine the curves of all panels in Figure 3. These curves are color-coded by the ranges of R. Figure 4b shows the mean Φ^W as a function of R for various ranges of u. It is observed that Φ^W decreases with increasing R up to 16 Re. In the region with R > 16Re, Φ^W does not increase with increasing R. This is possibly due to additional heating mechanisms for electrons and ions.

Since the simulations by Engwall et al. (2006) were performed only for u = 20km/s, it is more illustrative to use Φ^W to estimate r_T for u between 17.5 and 22.5 km/s rather than other u ranges. As demonstrated by the solid light blue curve in Figure 4b, the mean value of Φ^W with R between 6 and 8 Re is approximately 0.67 V. In places with R between 18 and 20 Re within the same u range, the mean value of Φ^W decreases to approximately 0.40 V. According to the simulation results of Engwall et al. (2006), which are listed in Table 1, Φ^W of 0.60 and 0.23 V correspond to r_T of 2

and 0.5, respectively. For r_T of 1, simulations with four combinations of ion and electron temperatures yield the values of Φ^W from 0.32 to 0.39 V. Therefore, we conclude that r_T decreases from > 2 to approximately 1 as the cold plasma flows into the tail lobes.

For other values of u, it is also observed that Φ^w decreases with increasing R up to 16 Re. This indicates that r_T basically decreases as the cold plasma moves into the tail lobes. At $R = [16,20) \,\text{Re}$, r_T seems to be positively correlated with R. This may be explained by more efficient heating of electrons than ions in the far-tail regions.

5 Discussion

As mentioned in Section 2, our method uses a comparison of the measured Φ^W values with the simulated values. The simulations used discrete values of parameters, including u, T_e , T_i , V_{SC} , and n_0 . Although it is not accurate to quantify the exact values of r_T , simulations with discrete values allow us to infer correlation relationships.

In general, the ion temperature is not necessarily the same as the electron temperature in the collisionless plasma of the tail lobes. Although there is no direct measurement of temperatures for both ions and electrons of cold plasma from the Cluster mission, our observation of the anti-correlation between r_T of cold plasma in the lobes and R indicates that the ions and the electrons are heated differently during their transport.

In the solar wind, the temperature ratio also varies with the increasing distance from the Sun. Shi et al. (2023) used the measurements from the Parker Solar Probe (PSP) below 30 solar radii and from the WIND at 1 AU. They found that the electron-to-proton temperature ratio evolves as the solar wind propagates

from the Sun to the Earth. The observation is compared to their simulations, suggesting that the changes in the temperature ratio depend on the portion of the dissipated Alfvén wave energy that heats the protons or electrons. Their work suggests that Alfvén waves are one possible explanation for the evolution of proton and electron temperatures in the solar wind.

To explain the anti-correlation between r_T and R for cold plasma escaping from the ionosphere, we consider that the Alfvén wave in the lobes may play an important role [see a review by Keiling (2009)] because Alfvén waves are observed to interact with outflowing ions in the lobe (Sauvaud et al., 2004). In the lobes, the magnetic field lines act as a guide field for Alfvén waves. Because the wave frequencies overlap the gyrofrequencies of the cold ions, ions are considered to be heated more than electrons are. As R increases, the ion temperature increases more than the electron temperature. This explains the existence of the anti-correlation. A simulation on this is out of scope in the current data report and requires future work.

In Figure 4b, the violation of the anti-correlation is observed in R > 16Re and is nearly constant in Φ^W in R > 13Re for u > 22.5 km/s. Both phenomena may be explained by additional heating mechanisms that favor electrons near the plasma sheet boundary layer (PSBL), where cold plasma can be affected by the dipolarization fronts (DFs).

In general, electrons have a gyroradius much smaller than the scale thickness of the DF. Electrons are well magnetized and efficiently heated/accelerated by betatron acceleration due to the compression of magnetic flux in the DF (Fu et al., 2012; Gabrielse et al., 2016; Runov et al., 2013; Xu et al., 2018). Ions are often demagnetized and are less affected by DFs. This explanation is consistent with the fact that Cluster spacecraft were in the vicinity of the PSBL at large R.To verify this explanation, a follow-up study is needed to investigate the association of the DFs with the enhanced Φ^W in the tail.

6 Conclusion

In this study, the electric-field measurements of the plasma wake, formed by the Cluster spacecraft as it interacts with cold plasma escaping from the ionosphere, are used to examine how the electron-to-ion temperature ratio evolves as cold plasma flows into the tail lobes for the first time. Our findings are as follows.

- At the same distance from the Earth, we observe a correlation between the wake potential and the plasma flow speed, which aligns with theoretical predictions.
- For a constant plasma flow speed, the electron-to-ion temperature ratio decreases with increasing distance from the Earth up to 16 Re, suggesting a heating mechanism that favors ions in the lobes.
- Beyond 16 Re, the increasing ratio suggests that electrons experience greater heating than ions.

Data availability statement

Publicly available datasets were analyzed in this study. These data can be found at http://cosmos.esa.int/web/csa.

Author contributions

KL: Project administration, Methodology, Validation, Visualization, Conceptualization, Funding acquisition, Writing – original draft, Formal analysis, Writing – review and editing, Supervision, Resources, Investigation, Data curation, Software. JC: Software, Visualization, Writing – review and editing, Validation. LC: Methodology, Investigation, Writing – review and editing, EK: Funding acquisition, Writing – review and editing, Methodology, Formal analysis, Investigation. ND: Writing – review and editing, Funding acquisition.

Funding

The authors declare that financial support was received for the research and/or publication of this article. This work is funded by the Guangdong Basic and Applied Basic Research Foundation under grants 2023A1515010887. KL, EK, and ND acknowledge the LMU-China Academic Network for the support. EK is also funded by the DFG Heisenberg under grant number 516641019. ND is supported by DFG project number 520916080.

Acknowledgements

KL thanks Anders Eriksson and Mats André at the Swedish Institute of Space Physics for a helpful discussion.

Conflict of interest

The authors declare that the research was conducted in the absence of any commercial or financial relationships that could be construed as a potential conflict of interest.

Generative Al statement

The authors declare that no Generative AI was used in the creation of this manuscript.

Any alternative text (alt text) provided alongside figures in this article has been generated by Frontiers with the support of artificial intelligence and reasonable efforts have been made to ensure accuracy, including review by the authors wherever possible. If you identify any issues, please contact us.

Publisher's note

All claims expressed in this article are solely those of the authors and do not necessarily represent those of their affiliated organizations, or those of the publisher, the editors and the reviewers. Any product that may be evaluated in this article, or claim that may be made by its manufacturer, is not guaranteed or endorsed by the publisher.

References

Alpert, Y. L., Gurevich, V. G., and Pitaevskii, P. L. (1965). Space physics with artificial satellite. Consultants Bureau.

André, M., Li, K., and Eriksson, A. I. (2015). Outflow of low-energy ions and the solar cycle. *J. Geophys. Res. Space Phys.* 120, 1072–1085. doi:10.1002/2014JA020714

André, M., Eriksson, A. I., Khotyaintsev, Y. V., and Toledo-Redondo, S. (2021). The spacecraft wake: interference with electric field observations and a possibility to detect cold ions. *J. Geophys. Res. Space Phys.* 126, e29493. doi:10.1029/2021JA029493

Axford, W. I. (1968). The polar wind and the terrestrial helium budget. *J. Geophys. Res.* 73, 6855–6859. doi:10.1029/JA073i021p06855

Balogh, A., Carr, C. M., Acuña, M. H., Dunlop, M. W., Beek, T. J., Brown, P., et al. (2001). The cluster magnetic field investigation: overview of in-flight performance and initial results. *Ann. Geophys.* 19, 1207–1217. doi:10.5194/angeo-19-1207-2001

Collinson, G. A., Glocer, A., Pfaff, R., Barjatya, A., Conway, R., Breneman, A., et al. (2024). Earth's ambipolar electrostatic field and its role in ion escape to space. *Nature* 632, 1021–1025. doi:10.1038/s41586-024-07480-3

Engwall, E., Eriksson, A. I., and Forest, J. (2006). Wake formation behind positively charged spacecraft in flowing tenuous plasmas. *Phys. Plasmas* 13, 062904. doi:10.1063/1.2199207

Engwall, E., Eriksson, A. I., Cully, C. M., André, M., Torbert, R., and Vaith, H. (2009). Earth's ionospheric outflow dominated by hidden cold plasma. *Nat. Geosci.* 2, 24–27. doi:10.1038/ngeo387

Fu, H. S., Khotyaintsev, Y. V., Vaivads, A., André, M., and Huang, S. Y. (2012). Electric structure of dipolarization front at sub-proton scale. *Geophys. Res. Lett.* 39, L06105. doi:10.1029/2012GL051274

Gabrielse, C., Harris, C., Angelopoulos, V., Artemyev, A., and Runov, A. (2016). The role of localized inductive electric fields in electron injections around dipolarizing flux bundles. *J. Geophys. Res. Space Phys.* 121, 9560–9585. doi:10.1002/2016 IA023061

Gustafsson, G., Bostrom, R., Holback, B., Holmgren, G., Lundgren, A., Stasiewicz, K., et al. (1997). The electric field and wave experiment for the cluster mission. *Space Sci. Rev.* 79, 137–156. doi:10.1023/A:1004975108657

Haaland, S., Eriksson, A., Engwall, E., Lybekk, B., Nilsson, H., Pedersen, A., et al. (2012). Estimating the capture and loss of cold plasma from ionospheric outflow. *J. Geophys. Res. Space Phys.* 117, A07311. doi:10.1029/2012JA017679

Keiling, A. (2009). Alfvén waves and their roles in the dynamics of the Earth's Magnetotail: A Reviewm *Space Sci. Rev.* 142, 73–156. doi:10.1007/s11214-008-9463-8

Keiling, A., Parks, G. K., Wygant, J. R., Dombeck, J., Mozer, F. S., Russell, C. T., et al. (2005). Some properties of Alfvén waves: Observations in the tail lobes and the plasma sheet boundary layer. *J. Geophys. Res. Space Phys.* 110, A10S11. doi:10.1029/2004JA010907

Li, K., André, M., Eriksson, A., Wei, Y., Cui, J., and Haaland, S. (2021). High-latitude cold ion outflow inferred from the Cluster wake observations in the magnetotail lobes and the polar cap region. *Front. Phys.* 9, 620. doi:10.3389/fphy.2021.743316

Nilsson, H., Engwall, E., Eriksson, A., Puhl-Quinn, P. A., and Arvelius, S. (2010). Centrifugal acceleration in the magnetotail lobes. *Ann. Geophys.* 28, 569–576. doi:10.5194/angeo-28-569-2010

Paschmann, G., Quinn, J. M., Torbert, R. B., Vaith, H., McIlwain, C. E., Haerendel, G., et al. (2001). The Electron Drift Instrument on Cluster: overview of first results. *Ann. Geophys.* 19, 1273–1288. doi:10.5194/angeo-19-1273-2001

Rème, H., Aoustin, C., Bosqued, J. M., Dandouras, I., Lavraud, B., Sauvaud, J. A., et al. (2001). First multispacecraft ion measurements in and near the earth's magnetosphere with the identical cluster ion spectrometry (cis) experiment. *Ann. Geophys.* 19, 1303–1354. doi:10.5194/angeo-19-1303-2001

Runov, A., Angelopoulos, V., Gabrielse, C., Zhou, X.-Z., Turner, D., and Plaschke, F. (2013). Electron fluxes and pitch-angle distributions at dipolarization fronts: THEMIS multipoint observations. *J. Geophys. Res. Space Phys.* 118, 744–755. doi:10.1002/jgra.50121

Sauvaud, J. A., Louarn, P., Fruit, G., Stenuit, H., Vallat, C., Dandouras, J., et al. (2004). Case studies of the dynamics of ionospheric ions in the Earth's magnetotail. *J. Geophys. Res. Space Phys.* 109, A01212. doi:10.1029/2003JA009996

Shi, C., Velli, M., Lionello, R., Sioulas, N., Huang, Z., Halekas, J. S., et al. (2023). Proton and Electron Temperatures in the Solar Wind and Their Correlations with the Solar Wind Speed. *ApJ* 944, 82. doi:10.3847/1538-4357/acb341

Takada, T., Nakamura, R., Baumjohann, W., Seki, K., Vörös, Z., Asano, Y., et al. (2006). Alfvén waves in the near-PSBL lobe: Cluster observations. *Ann. Geophys.* 24, 1001–1013. doi:10.5194/angeo-24-1001-2006

Xu, Y., Fu, H. S., Liu, C. M., and Wang, T. Y. (2018). Electron Acceleration by Dipolarization Fronts and Magnetic Reconnection: A Quantitative Comparison. *ApJ* 853, 11. doi:10.3847/1538-4357/aa9f2f